Quartz to Stishovite: Wave Propagation in the Mixed Phase Region

D. E. GRADY, W. J. MURRI, AND G. R. FOWLES

Poulter Laboratory, Stanford Research Institute
Menlo Park, California 94025

This work reports on phase transition kinetics and wave propagation in Arkansas novaculite, a fine-grained polycrystalline α quartz rock, when it is subject to high-pressure dynamic loading and relief. The stress region studied is between 150 and 400 kbar, where the polymorphic phase transition from α quartz to stishovite is believed to occur. Particular emphasis was focused on the unloading behavior in the mixed phase region. High-pressure loading is provided by conventional explosive methods. Measurements of the transient flow field are obtained with in-material manganin stress gages or magnetic particle velocity gages. Results showed partial transformation to the high-density phase occurring in the shock front, the degree of transformation depending on peak driving stress. A continuing transformation rate behind the shock front is very small, i.e., at least 3 orders of magnitude slower than the initial transformation rate. Unloading from stress-volume points in the mixed phase region is observed to occur along, or close to, paths of frozen phase concentration down to approximately 80 kbar. Below this stress the data indicate a transition of the high-density phase to a lower-density phase.

The present work reports on an investigation of Arkansas novaculite, a naturally occurring polycrystalline α quartz rock, when it is subject to shock wave loading. The pressure region studied is between 150 and 400 kbar, within which the polymorphic transformation of α quartz to stishovite has been reported to occur. Of primary interest is the unloading behavior of the material.

In earlier work, attention has focused on the shock wave properties of quartz for several reasons. Since it is pure silicon dioxide in a structure of silicon in tetrahedral coordination with oxygen and since this is the fundamental building block of more complex silicate minerals, understanding of the behavior of quartz is prerequisite to that of the more complicated minerals. One line of geophysical interest has stemmed from observation of mineral content in the vicinity of meteorite craters, where several polymorphs of high-density quartz have been uncovered [*Chao et al.*, 1962]. It is believed that they originated as a result of shock metamorphoses during meteorite impact. Further geophysical interest is provided by a quest to understand the mineral composition and polymorphic structure of the earth's mantle [*Wang*, 1968; *Anderson and Kanamori*, 1968; *Ahrens et al.*, 1969]. Pure silicon dioxide exhibits a high-pressure polymorphic phase transition, which is possibly representative of the expected behavior of most of the candidate mantle silicates. Quartz and other silicates and silicate-bearing rock constitute a large portion of the earth's surface, and accurate prediction of energy coupling and dynamic wave propagation in the vicinity of high velocity or explosive impact also requires studies of this kind.

Single-crystal and amorphous quartz were extensively investigated under shock loading by *Wackerle* [1962] to about 700 kbar. He observed an anomalous compression in the region from 150 to 400 kbar. An independent static investigation of quartz identified a high-density polymorph [*Stishov and Popova*, 1961]. *McQueen et al.* [1963] concluded that stishovite was formed under shock compression and formulated a high-pressure equation of state from the shock wave results. Further shock wave studies by *Fowles* [1967] on single-crystal quartz provided more complete data in the region below and slightly above the Hugoniot elastic limit of the material. *Ahrens and Rosenberg* [1968] studied Arkansas novaculite and single-crystal quartz under shock loading in the mixed phase region and estimated the unloading response by observing the shock states transmitted by the quartz into liquid buffers. Recently, *Trunin et al.* [1971] have investigated quartz of varying porosity under shock loading in and above the mixed phase region. Their results for the lowest-density specimens strongly suggest that the extremely high temperatures developed may have induced transformation to the coesite phase. This interpretation has been questioned by *Davies* [1972]. He suggested shock-induced melting as an alternative process.

The experiments performed in the current work focus on the stress region from slightly above the Hugoniot elastic limit to about 400 kbar. The experimental data were obtained from two types of experiments. In the first, aluminum or magnesium flyer plates thrown by explosive systems impacted targets of Arkansas novaculite. Shock loading resulted from impact, and relief occurred by shock reflection from the flyer plate free surface. Manganin stress gages provided records of stress-time histories at increasing distance from the impact surface.

In the second type of experiment, Arkansas novaculite was loaded by in-contact explosive. Material unloading occurred initially by the Taylor relief wave originating behind the explosive detonation front. Subsequent relief to zero stress occurs from the reflection of the shock wave off the novaculite free surface. Initial unloading rates were several orders of magnitude lower than those obtained in the flyer plate experiments. In this type of experiment, magnetic particle velocity gages provided records of particle velocity history at different material points. The experimental objective was to determine whether the α quartz to stishovite transition continued, at some reduced rate, behind the shock front.

The stress-time and particle velocity-time data were analyzed by a method suggested by *Fowles and Williams*

[1970] and later extended by *Cowperthwaite and Williams* [1971]. The technique provides a means of mapping the data into the stress-volume and stress-particle velocity plane.

The results of this work can be summarized as follows:

1. Complete stress-time and particle velocity–time histories have been measured in quartz rock subject to high-pressure dynamic loading and relief.
2. Loading into the mixed phase region occurs by two shock waves for stresses below about 400 kbar. Partial transformation to the high-density phase occurs in the final shock front. The degree of transformation depends on the peak driving stress.
3. An effort was made to determine a continuing transformation rate after initial shock loading. We determined that it had to be at least 3 orders of magnitude lower than the initial transformation rate in the shock front.
4. Dynamic unloading from pressure-volume points in the mixed phase region is shown to occur along, or close to, paths of frozen phase concentration down to about 80 kbar.
5. Below 80 kbar a reverse phase transition of the high-density material to a lower density is suggested by the data. The phase transition appears to be rate-dependent with a characteristic time of the order of $\frac{1}{3}$ μs.

EXPERIMENTAL PROCEDURE

The novaculite used in these experiments was obtained from Norton Company of Littleton, New Hampshire. This material is a white, homogeneous, cryptocrystalline quartz rock with a grain size of about 0.01-mm diameter and nearly zero porosity. The longitudinal sound speed was measured as 5.9 mm/μs, and the density of our specimens was 2.63 g/cm^3.

Manganin stress gage system. Dynamic loading was provided by impact from explosively driven flyer plates on samples of the test material, as is indicated in Figure 1. Unloading occurred from the back surface of the flyer plate. Peak loading stress is controlled by flyer plate velocity. The flyer plate velocity was determined by the type and mass of the explosive and the flyer plate material and thickness. The flyer plate materials used in the present work were aluminum and magnesium. Flyer plate thicknesses were 0.63 and 1.0 cm.

Target samples of the various rock materials were 15 by 25 cm rectangular slabs 0.15–1.25 cm thick. Stress gages were mounted between slabs of material, two gages per plane in each of three planes. The back slab was sufficiently thick to ensure that relief occurred only from the flyer plate free surface. Gages lay along the large dimension and continued out the ends. The 25-cm dimension exceeded the diameter of the flyer plate by 5 cm. This precaution increased gage lifetime by reducing shearing strains in the vicinity of gage leads exiting from the rock sides.

Stress gages were photoetched from 50-μ manganin foil. The 1-Ω four-lead grid was approximately 1.5 cm square. Copper foil leads were soldered to the gage element to provide connection to the external circuit. The remainder of the volume in the gage plane was filled with C-7 epoxy. Final thickness of the gage plane was 50–75 μ.

Gage current excitation of about 5 A was provided by a constant current manganin gage supply [*Keough*, 1968]. Output was recorded via RG213 transmission cable on oscilloscopes in a differential mode. Frequency response rise time of the electronic system was approximately 0.01 μs. An additional high-frequency limitation occurred owing to pressure equilibration in the 50- to 75-μ-thick gage plane. A rise time can be estimated from the mechanical impedance properties of the gage plane epoxy [*Keough*, 1968] and the rock material. In the present work this was about 0.035 μs.

The gage material used in the present work was as-received Driver Harris foil. The loading calibration coefficient used was a cubic pressure-resistance expression provided by *Lyle et al.* [1969]. The calibration data are comparable with, but showed less scatter than, similar data obtained by *Keough* [1968].

On unloading, 20–30% residual change was observed on all stress data in this work, consistent with work reported by *Rosenberg and Ginsberg* [1972]. They have shown that prior work hardening of the gage material significantly reduces the observed residual resistance but an equivalent reduction in the loading coefficient also occurs. In the present work, as-received manganin was used, and a linear unloading calibration was assumed with the residual resistance level set to zero stress. The calibration used was:

Loading

$$\sigma = \alpha(\Delta R/R) + \beta(\Delta R/R)^2 + \gamma(\Delta R/R)^3 \qquad (1a)$$

Unloading

$$\sigma = \sigma_{max}(\Delta R/R - \Delta R/R_{res})/(\Delta R/R_{max} - \Delta R/R_{res}) \qquad (1b)$$

$$\alpha = 3.7 \times 10^2 \quad \beta = -1.32 \times 10^{+1} \quad \gamma = 4.42 \times 10^{+1}$$

where σ_{max} is the pressure obtained at $\Delta R/R_{max}$ and $\Delta R/R_{res}$ is the residual resistance change after unloading. Stress records in softer rock material have been obtained in which no residual resistance is observed. We have found no explanation and must conclude that complete understanding of gage behavior on unloading from high stress levels is still not available.

One further point about calibration: although care was taken to select a flyer plate material that is of lower impedance than the rock on unloading, achievement of this cannot be verified before the fact. Unloading to zero stress in one reverberation is provided by this precaution. Final proof that the unloading to zero stress occurred was provided by the pressure–particle velocity curves obtained from the analyzed data after the fact. Results showed that the quartz on unloading has higher impedance.

Particle velocity gage system. In experiments using magnetic particle velocity gages as the recording transducer [*Dremin and Shvedov*, 1964; *Edwards et al.*, 1970], dynamic loading was provided by in-contact explosive systems. Stress unloading was allowed to proceed in two ways. First, a Taylor wave, originating in the explosive gases, provided a rather gentle unloading behind the shock front. The magnitude of this unloading depends on the stiffness of the test material; it is of the order of 5–10% over several microseconds in the novaculite. Useful conclusions were obtained concerning the high-pressure behavior of quartz using the Taylor unloading wave. Second, a more rapid relief was provided by reflecting the induced shock wave off the free surface of the sample.

Target construction followed the procedure discussed

previously for stress gages. The U-shaped gages were photoetched from 50-μ copper foil. Ribbon width was 1.5 mm. The center-to-center active element gage length was 11.6 mm. Gages were mounted between slabs of rock and on the free surface along the greater length of the target. Pulsed Helmholtz coils provided a uniform quasi-static magnetic field for the duration of the experimental measurement ($\sim$5 μs). General description of the method used was given by *Murri* [1972]. The target assembly was located between the Helmholtz coils so that the volume traversed by the active element gage during the shock was in the center of the uniform flux region. Gage output was recorded differentially by cathode ray oscilloscopes. Voltage-time profiles $\mathcal{E}(t)$ were reduced to particle velocity–time $u(t)$ through the relation

$$u(t) = \mathcal{E}(t)/lB \qquad (2)$$

where l is the center-to-center active gage length and B is the magnetic field.

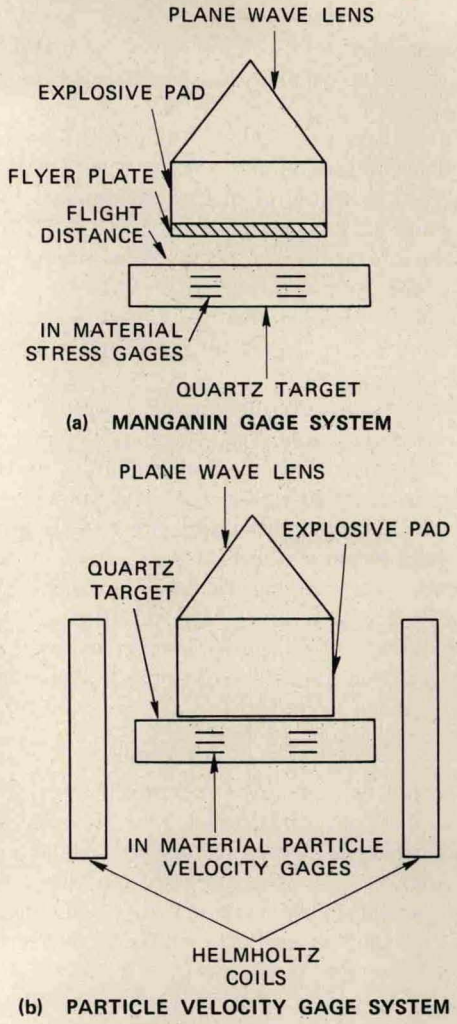

Fig. 1. Experimental systems.

Analysis and Interpretation

Stress gage experiments. A set of manganin gage stress-time profiles obtained in one flyer plate experiment in Arkansas novaculite is shown in Figure 2 along with the experimental configuration. The profile dispersion at increasing distance from the impact surface can be seen from consecutive gage records. Two gages in each plane show the reproducibility of gage response. Four experiments of this type were performed.

In the loading portion a two-wave structure was observed in all but the 440-kbar peak stress experiment. The first wave is associated with yielding at the Hugoniot elastic limit in polycrystalline quartz and propagates with a velocity of about 6.1 mm/μs. In experiments where a two-wave structure was observed on loading, a tendency for the stress amplitude of the first wave to decay with propagation distance was noted. The amount of attenuation was about 4–5 kbar over the 6-mm propagation distance from the first to third gage plane. This stress-relaxing effect has been discussed by *Ahrens and Duvall* [1966]. The attenuation observed was of the order of the scatter in the data, and the Hugoniot elastic limit values stated in Table 1 are an average of this behavior.

The second wave, loading the material to peak stress, provides the final Hugoniot state in Table 1. In the 440-kbar peak stress experiment the elastic precursor was overdriven and thus not observed. The elastic and final state Hugoniot data obtained in the present work are shown in Figure 3. They are in agreement with previous shock wave data on quartz [*Ahrens and Rosenberg*, 1968; *Wackerle*, 1962].

The propagation characteristics of the unloading wave in polycrystalline quartz are also seen in the stress-time profiles in Figure 2. The average relief wave velocity is considerably faster than the loading wave velocity and indicates strongly dissipative wave propagation. Pronounced dispersion is shown by spreading of the relief wave in consecutive profiles.

The sharp break in the relief wave seen in Figure 2 was observed in all stress gage experiments. It occurred at approximately 80 kbar, regardless of peak stress. It is not a phenomenon associated with the manganin gage material. Similar records obtained in other rock material fail to show this behavior. We believe that the break in the relief wave is associated with a reverse transition of high-density quartz to a lower-density material during unloading. The behavior of the stress wave propagation in the lower region of the relief profile does not appear to be forming a rarefaction shock. There appears rather to be a break in slope in individual records and a faster dispersion of the wave in this region. This would be the wave structure expected if transition to a lower-density phase were occurring with a finite relaxation time. A rough calculation assuming a simple stress-relaxing solid results in a relaxation time constant of the order of $\frac{1}{3}$ μs. The poorer quality of profiles in this region prohibited a more detailed study.

According to the method of analysis developed originally by *Fowles and Williams* [1970] and extended by *Cowperthwaite and Williams* [1971], multiple-stress gages providing stress-time histories at neighboring Lagrangian coordinates are sufficient to determine the stress-volume path of a material element within the region of the gages. Velocities C_σ and C_u of constant stress or particle velocity levels are estimated from the data and in conjunction with the equation of mass and momentum are used to determine the stress-volume paths. This analysis provided relief adiabats in the mixed phase region. In the present work a dependence of C_σ on the Lagrangian coordinate h could not be determined. In the event that C_σ is a function of σ only and propagation

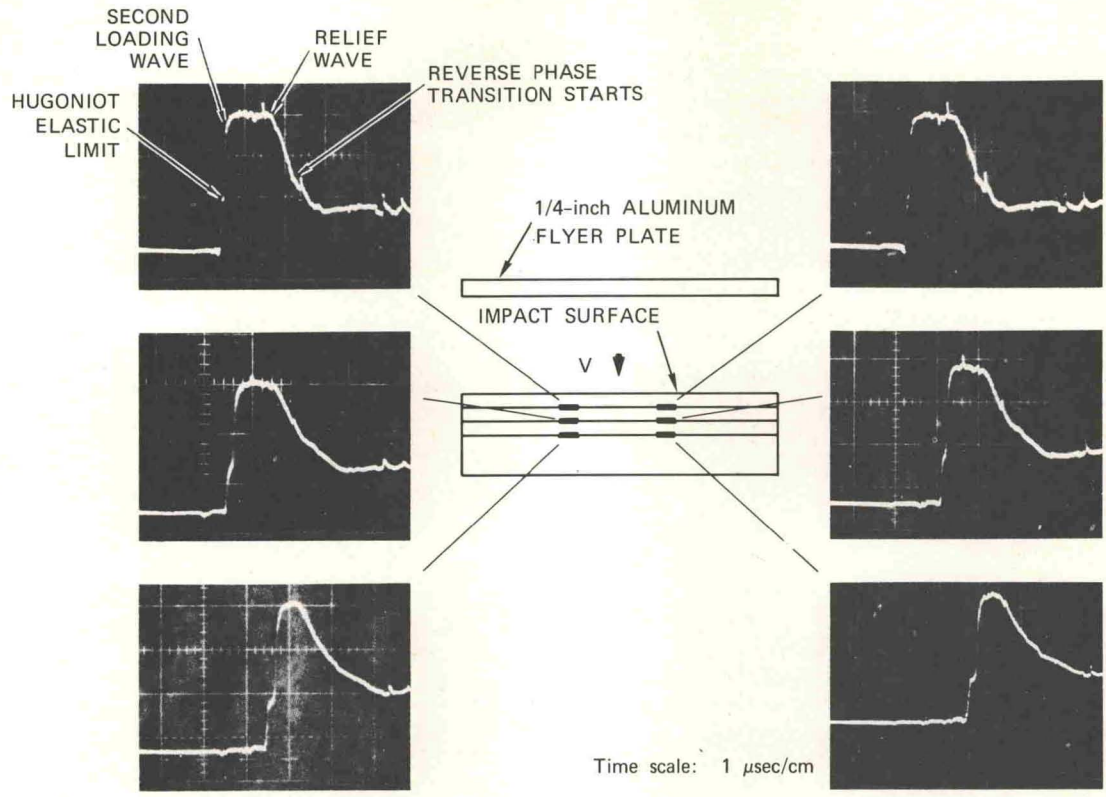

Fig. 2. Manganin stress gage profiles in Arkansas novaculite. Peak stress of 252 kbar.

is into a region of constant state (simple wave) $C_\sigma = C_u = C$ and the stress volume history reduces to a single integral [*Cowperthwaite and Williams*, 1971],

$$V = V_H - \int_{\sigma_H}^{\sigma} \frac{d\sigma}{\rho_0^2 C^2} \tag{3}$$

Time correlation between experimental records was a weak point in the present work and the primary source of scatter in the Hugoniot data points shown in Figure 3. Before (3) was used to determine unloading behavior of the material, the present Hugoniot data with those of *Ahrens and Rosenberg* [1968] and *Wackerle* [1962] in the mixed phase region were fit to an analytic function. The fitted Hugoniot is shown in Figure 3 as a solid line. This Hugoniot was used to provide better time correlation between experimental profiles. This procedure is reasonable. Values for the shock velocity in this stress region are not in question. It is the relief velocities as a function of stress that determine the unloading path.

TABLE 1. Arkansas Novaculite: Shock Wave Data

	Elastic				Plastic			
Shot	C_e, mm/μs	σ_e,* kbar	U_e, mm/μs	V_{hel}, cm³/g	U_s, mm/μs	σ_H, kbar	U_H, mm/μs	V_H, cm³/g
8909-1†	...	...	...	...	6.3	444	2.60	0.218
1883-4	6.20	90	0.552	0.346	5.40	252	1.94	0.268
1883-16	6.05	95	0.597	0.343	5.45	352	2.39	0.218
1883-17	6.24	85	0.52	0.348	5.70	222	1.43	0.287
1883-6	6.20	70	0.425	0.135	5.60	241	1.63	0.272
1883-7	6.00	98	0.62	0.341	5.50	252	1.68	0.268
8909-2	6.03	79	0.50	0.349	5.45	301	2.10	0.234

*Average of six gages (trend of decay with distance ~4-5 kbar over 6 mm).
†Elastic wave was overdriven.

The complete stress-volume paths are shown in Figure 4. The Hugoniot jump conditions were used to determine the loading paths, and (3) was used to determine the relief path.

It was assumed that the quartz relieved to zero stress after shock reflection from the aluminum flyer free surface. The assumption is reasonable, since the quartz relief adiabats determined from this work are steeper than similar adiabats for aluminum. No experiments were performed to justify this assumption. If the manganin gage level after relief corresponded to some residual stress, the effect on the predicted relief path would be small at the top of the relief and would become progressively more pronounced at lower stresses. The overall effect would be to shift the unloading paths slightly to the right in Figure 4. Also, the predicted level at which the reverse phase change is expected to proceed would be higher (~120 kbar). The best indication that a stress level close to zero was obtained upon first relief comes from the gage records. A number of gages survived a sufficient length of time to have shown a second reverberation relief from the flyer free surface; no clear indication of a second relief wave was observed.

The steep relief behavior in quartz has been observed in earlier work by *Ahrens and Rosenberg* [1968], where optical methods and shock reflection techniques provided estimates of the relief behavior. *Butkovich* [1971] found that prediction of peak stress attenuation with range in the Benham event required large hysteresis in the constitutive model of the quartz rock. The present work provides independent corroboration of this previous work.

In Figure 4, principal isentropes (hydrostatic) for α quartz and stishovite are shown. The isentrope shown for

α quartz is a Murnaghan equation fit to acoustic data [*Anderson*, 1966] and is consistent with static data of *McWhan* [1967]. The α quartz isentrope has been extrapolated beyond the pressure at which α quartz is expected to undergo polymorphic phase transformation to stishovite. The stishovite isentrope shown is also a Murnaghan equation fit. The parameters were determined by *Ahrens et al.* [1970] from shock wave and thermodynamic data. These isentropes determine the region of mixed phase in the pressure-volume plane.

To understand the unloading behavior in the mixed phase region, three curves of frozen concentration corresponding to 25, 50, and 75% stishovite are shown. The curves were obtained by constant specific volume ratios between the principal isentropes of α quartz and stishovite. Thermodynamically, pressure, temperature, and particle velocity equilibriums are assumed between phases, and surface energies are ignored. Although the lever rule is strictly valid only for isotherms, differences between α quartz and stishovite isotherms and isentropes are negligible up to pressures better than 300 or 400 kbar. Finally, the principal isentrope for stishovite shown in Figure 4 and that reached under shock compression from the α quartz initial specific volume differ slightly. Despite the number of assumptions required the curves obtained are reasonably close to paths of frozen concentration and provide a reference frame for examining the experimental unloading behavior. Our conclusion is that after partial or complete transformation to the high-density phase, material unloading occurs along, or close to, paths of frozen concentration down to about 80 kbar.

Particle velocity gage experiments. The previous experiments using flyer plate impact do not indicate a continuing quartz to stishovite phase transformation after the initial shock has placed the material in the mixed quartz-stishovite metastable region. The in-contact explosive experiments provided an unloading rate, after shock loading, substantially less than that obtained in the flyer plate experiments. We attempted to observe a continuing phase transformation rate within this longer experimental time scale.

The Taylor wave produces a decaying triangular particle velocity profile in the material, as the profiles obtained from one of two similar experiments shown in Figure 5 indicate. The initial unloading rate observed was about 10 kbar/μs, or better than 2 orders of magnitude lower than unloading rates in the flyer plate experiments. The sudden acceleration observed in Figure 5 occurs when the relief wave from the target free surface reaches the gage planes.

In Figure 6, three particle velocity profiles are shown that idealize the experimental data during initial unloading. The particle velocity field is determined by the shock velocity U, the slope of individual profiles a, and the slope of the decaying shock front b. The following analysis determines the initial unloading stress-volume path in the mixed phase region in terms of these parameters. Comparison with paths of frozen quartz-stishovite phase concentration determines whether the α quartz to stishovite transformation is continuing behind the shock front in the time span of the Taylor relief wave.

The particle velocity field behind the shock can be written

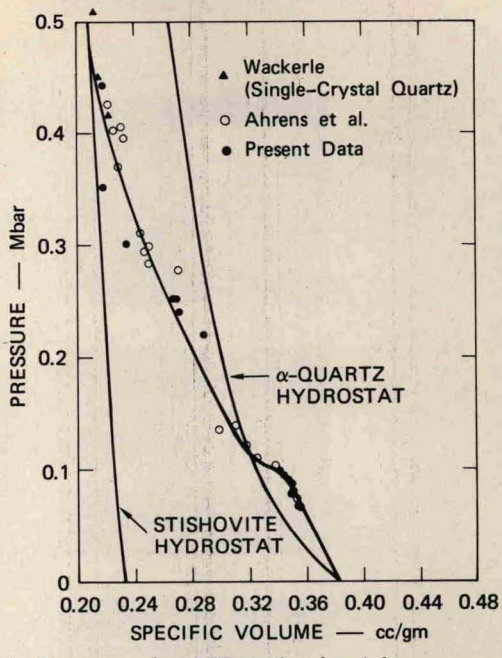

Fig. 3. Pressure-volume Hugoniot for Arkansas novaculite.

$$u(h, t) = u_0 + at + \frac{b - a}{U} h \tag{4}$$

where u_0 is the initial particle velocity magnitude of the first profile at zero time (arrival of the shock wave at the first gage) and h is the Lagrangian coordinate. The initial stress-volume path can be determined by obtaining the velocities of constant stress and particle velocity levels C_σ and C_u and using the relation [*Fowles and Williams*, 1970]

$$d\sigma/dV = -\rho_0^2 C_u C_\sigma \tag{5}$$

Equation 6 is obtained by using (4) and $C_u = (\partial h/\partial t)_u$:

$$C_u = \frac{a}{a - b} U \tag{6}$$

Equation 7 is obtained from (4) by using $C_\sigma = (\partial h/\partial t)_\sigma$ and the Hugoniot jump condition:

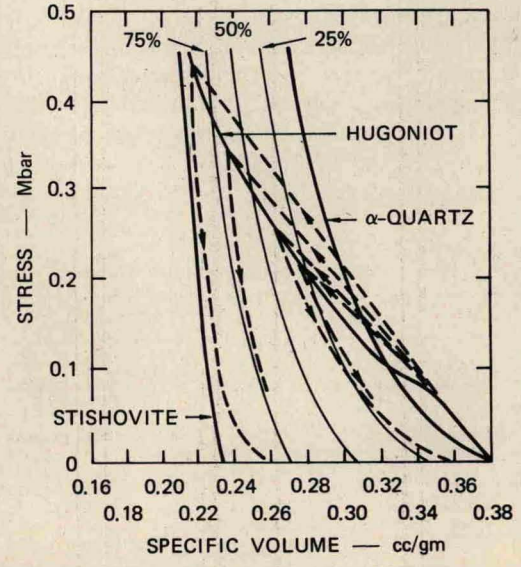

Fig. 4. Stress-volume relief paths in Arkansas novaculite. Loading and relief paths are indicated by the dashed lines.

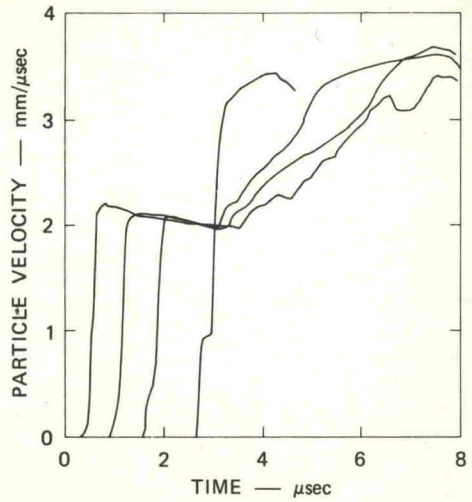

Fig. 5. Collective plot of four particle velocity profiles including one on the free surface in Arkansas novaculite shocked to a peak stress of 300 kbar.

$$C_\sigma = \left(1 + \frac{b}{a}\right) U \tag{7}$$

By using (5), the stress-volume path in the unloading region is determined.

$$\frac{d\sigma}{dV} = -\rho_0^2 \left(\frac{a + b}{a - b}\right) U^2 \tag{8}$$

Note that the values of C_σ and C_u can be quite unusual. For instance, $C_\sigma = 2U$ and $C_u = \infty$ correspond to stress unloading at constant volume.

Two experiments were performed with different thickness of explosive. The experimental parameters obtained from the data are given in Table 2. The errors in a and b are average values determined from ambiguity in the profiles. Errors in the shock velocity are small in comparison with errors in a and b. The quantity C is the acceleration wave velocity at which the foot of the relief wave from the free surface of the novaculite propagates (Figure 5). Values for U and C refer to Lagrangian or material coordinates.

To determine whether the quartz-stishovite phase transition is occurring behind the shock front, the stress-volume unloading path from the Hugoniot point in the mixed phase region is compared with the slope of the frozen concentration path. The slope of the frozen concentration curve is determined from the acceleration velocity C, a frozen sound speed being assumed, and is consistent with estimates from thermodynamic data.

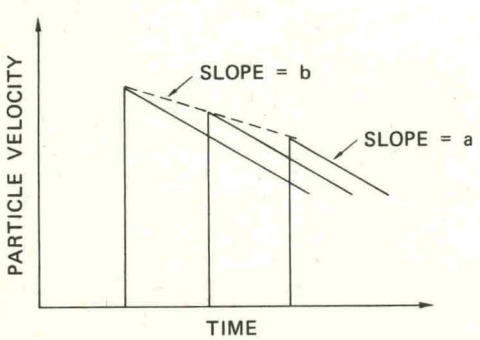

Fig. 6. Triangular wave profiles representing initial unloading behavior due to Taylor wave.

TABLE 2. Relief Wave Data

Shot	σ_H, kbar	U_H, mm/μs	U, mm/μs	C, mm/μs	a, mm/μs^2	b, mm/μs^2
8909-2	301	2.10	5.45	16.5	-0.090 ± 0.014	-0.09 ± 0.014
1883-6	241	1.63	5.65	12.4	-0.106 ± 0.02	-0.12 ± 0.04

The results for both experiments are shown in Figure 7. The error in a and b results in an uncertainty in the stress-volume path. Initial unloading is within the shaded cones shown in the figure. The dashed lines are slopes of frozen quartz-stishovite concentration curves. The data suggest a slight tendency toward the stishovite phase; however, within experimental error we conclude that unloading is along paths of constant concentration at the considerably lower unloading rates of these experiments. This result is the same as that obtained at a much higher unloading rate in the plate impact experiments.

DISCUSSION

In the present work, stress wave profiles have been measured that exhibit the nature of dynamic wave propagation in the high-pressure mixed phase region of quartz and stishovite. In particular, certain features of the shock-induced transition from α quartz to stishovite have been observed. The dynamic loading is characterized by a two-wave structure. The first wave is associated with mechanical yielding of the material. Application of the Hugoniot conservation relation to both loading waves places the material well into the mixed phase region. The partial phase transition apparently occurred within the final shock front. There is no indication in the observed loading profiles that the yielding process and the phase transition occur at different stress levels. Within the frequency response of the transducer system, no width was observed in the final load-

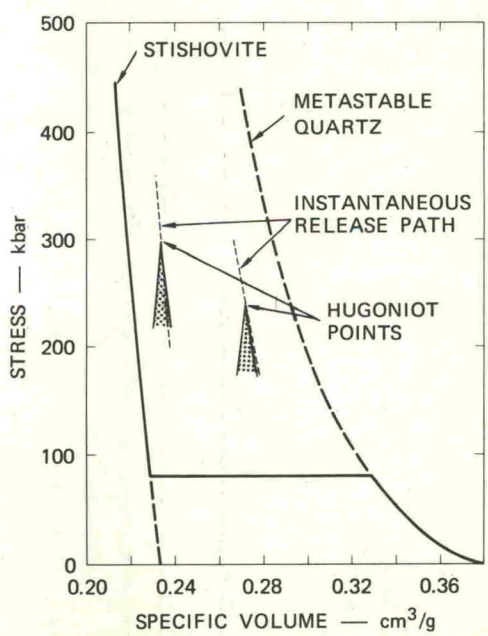

Fig. 7. Taylor wave unloading in Arkansas novaculite. The shaded area indicates the uncertainty in the experimental determination of the initial stress-volume release path behind the shock front.

ing wave that would indicate a relaxation time with the initial phase transition. It can be stated that the relaxation time is substantially less than 0.035 μs, which is the limit of resolution of the present system.

For stress levels less than about 430 kbar the transition ceases (or substantially reduces in rate) before complete stishovite density is reached. The proportion of material transformed depends on the peak stress attained behind the shock front. Experiments performed in this work indicate that the initial transformation rate (in the shock front) and the continuing transformation rate (behind the shock front) differ by at least 3 orders of magnitude.

Analyses of the present experimental results have shown that the pressure-volume behavior of the material during dynamic relief from states in the mixed phase region is along, or close to, paths of frozen concentration. This is a consequence of the extremely reduced transformation rate after initial shock loading.

The character of the measured profiles below about 80 kbar on unloading indicates that a transformation of the higher-density phase to a lower-density material is proceeding. This conclusion is consistent with recovery work of several authors. *Wackerle* [1962] observed amorphous quartz in one recovered specimen of shock-loaded quartz. Similar observations were made by *De Carli and Milton* [1965] on quartz sandstone, and analogous results have been obtained on quartz powder in a copper matrix by *Kleeman and Ahrens* [1973].

In the interpretation of the present results it has been tacitly assumed that strength effects could be ignored after yield occurred in the quartz material. Consistency of the present results with that assumption suggests that it is reasonable. Further justification is provided by the close agreement of stishovite initial density as determined from shock wave data and by measurement on stishovite samples.

Acknowledgments. The authors wish to express appreciation to the staff of Poulter Laboratory, especially M. Cowperthwaite, D. R. Curran, P. S. De Carli, and C. F. Petersen for many discussions with us and to B. Y. Lew and Fred Richey for patiently reading and analyzing the gage records, for computer programing, and for endless calculations. We wish to acknowledge the assistance of A. C. Wheeler, L. B. Hall, and D. Walter in preparing the experimental assemblies and the electronic and explosive instrumentation. We also wish to thank D. B. Larson of Lawrence Livermore Laboratory for his contributions in several discussions. This work was supported by the U.S. Atomic Energy Commission.

REFERENCES

Ahrens, T. J., and G. E. Duvall, Stress relaxation behind elastic shock waves in rocks, *J. Geophys. Res., 71,* 4349–4360, 1966.

Ahrens, T. J., and J. T. Rosenberg, Shock metamorphism: Experiments on quartz and plagioclase, in *Shock Metamorphism of Natural Materials,* edited by B. M. French and N. M. Short, pp. 59–81, Mono Book, Baltimore, Md., 1968.

Ahrens, T. J., D. L. Anderson, and A. E. Ringwood, Equations of state and crystal structures of high-pressure phases of shocked silicates and oxides, *Rev. Geophys. Space Phys., 7,* 667–707, 1969.

Ahrens, T. J., T. Takahashi, and G. F. Davies, A proposed equation of state of stishovite, *J. Geophys. Res., 75,* 310–316, 1970.

Anderson, D. L., and H. Kanamori, Shock-wave equations of state of rocks and minerals, *J. Geophys. Res., 73,* 6477–6502, 1968.

Anderson, O. L., The use of ultrasonic measurements under modest pressure to estimate compression at high pressure, *J. Phys. Chem. Solids, 27,* 547–565, 1966.

Butkovich, T. R., The influence of water in rocks on effects of underground nuclear explosions, *J. Geophys. Res., 76,* 1993–2011, 1971.

Chao, E. C. T., J. J. Fahey, J. Littler, and D. J. Milton, Stishovite, *Amer. Mineral., 46,* 807, 1962.

Cowperthwaite, M., and R. F. Williams, Determination of constitutive relationships with multiple gages in nondivergent flow, *J. Appl. Phys., 42,* 456–462, 1971.

Davies, G. F., Equation of state and phase equilibria of stishovite and a coesitelike phase from shock wave and other data, *J. Geophys. Res., 77,* 4920–4933, 1972.

De Carli, P. S., and D. J. Milton, Stishovite: Synthesis by shock wave, *Science, 147,* 144–145, 1965.

Dremin, A. N., and K. K. Shvedov, The determination of Chapman-Jouguet pressure and of the duration of reaction in the detonation wave of high explosives, *Zh. Prikl. Mekh. Tekh. Fiz., 2,* 154–159, 1964.

Edwards, D. J., J. O. Erkman, and S. J. Jacobs, The electromagnetic velocity gage and applications to the measurement of particle velocity in PMMA, NOLTR 70-79, 1970.

Fowles, R., Dynamic compression of quartz, *J. Geophys. Res., 72,* 5729–5742, 1967.

Fowles, R., and R. F. Williams, Plane stress wave propagation in solids, *J. Appl. Phys., 41,* 360–363, 1970.

Keough, D. D., Procedure for fabrication and operation of manganin shock pressure gage, *Tech. Rep. AFWL-TR-68-57,* Stanford Res. Inst., Menlo Park, Calif., 1968.

Kleeman, J. D., and T. J. Ahrens, The shock-induced transition of quartz to stishovite, *J. Geophys. Res., 78,* 5954, 1973.

Lyle, J. W., R. L. Shriver, and A. R. McMillan, Dynamic piezoresistive coefficient of manganin to 392 kbar, *J. Appl. Phys., 46,* 4663–4664, 1969.

McQueen, R. G., J. N. Fritz, and S. P. Marsh, On the equation of stishovite, *J. Geophys. Res., 68,* 2319–2322, 1963.

McWhan, D. B., Linear compression of α-quartz to 150 kbar, *J. Appl. Phys., 38,* 347–352, 1967.

Murri, W. J., Equation of state of rocks, final report, contract AT(04-3)-115, proj. 8909, Stanford Res. Inst., Menlo Park, Calif., 1972.

Rosenberg, J. T., and M. J. Ginsberg, Effect of cold work in piezoresistance of manganin foil, *Bull. Amer. Phys. Soc., 17,* 1078, 1972.

Stishov, S. M., and S. V. Popova, A new dense modification of silica, *Geokhimiya,* no. 16, 923–926, 1961.

Trunin, R. F., G. V. Simakov, and M. A. Podurets, Compression of porous quartz by strong shock waves, *Izv. Acad. Sci. USSR Phys. Solid Earth,* no. 2, 33–39, 1971.

Wackerle, J., Shock-wave compression of quartz, *J. Appl. Phys., 33,* 922–937, 1962.

Wang, C., Constitution of the lower mantle as evidenced from shock wave data for some rocks, *J. Geophys. Res., 73,* 6459–6476, 198.

(Received June 21, 1973;
revised October 11, 1973.)